JPEDAV (2004) 25:346-354
DOI: 10.1361/15477030420115
1547-7037/$19.00 ©ASM International

Reevaluation of the Fe-Mn Phase Diagram

V.T. Witusiewicz, F. Sommer, and E.J. Mittemeijer

(Submitted December 9, 2003; in revised form May 24, 2004)

New results for the enthalpy of mixing of liquid Fe-Mn alloys, the enthalpy of formation of γ-Fe-Mn solid solutions and the heat capacity of α-Fe-Mn and γ-Fe-Mn alloys obtained by isoperibolic calorimetry and differential thermal analysis (DTA) measurements have been used for the reassessment of the molar Gibbs energy of the various phases of the Fe-Mn system. Experimental information about martensitic transformation temperatures in Fe-Mn alloys published recently was incorporated in the updating of the occurring metastable equilibria. The present reevaluation results in a good fit with all available experimental data and is compared with the results of previous assessments.

1. Introduction

New experimental data for the enthalpy of formation of liquid and solid alloys and the heat capacity of solid α and γ-Fe-Mn alloys, have been published recently by the present authors [2003Wit]. Such data are crucial for the quantitative description the Fe-Mn phase diagram and for the assessment of the chemical driving forces of technically important solid-state transformations such as the fcc-A1(austenite)/bcc-A2(ferrite) and fcc-A1/cph-A3 martensitic phase transformations. The thermodynamic properties given in the existing CALPHAD descriptions [1987Hua, 1989Hua, 1989Lee, 1998COS] were updated in the present work on the basis of new experimental information on the enthalpy of mixing of liquid Fe-Mn alloys, the enthalpy of formation of γ-Fe-Mn solid solutions, the heat capacity of solid α-Fe-Mn and γ-Fe-Mn alloys provided by [2002Li, 2003Wit], and the martensitic transformation temperatures given by [1995Cot, 1998Cot]. To this end the least squares optimization module in Thermo-Calc called Parrot, as developed by Janson [1985Sun] was applied.

2. Experimental Data

As a basis for the assessment the main information on the phase equilibria was principally the same as selected by [1987Hua], [1989Hua] and [1989Lee], namely the high temperature phase equilibria from Hellawell and Hume-Rothery [1957Hel] and the low temperature fcc-A1/bcc-A2 phase equilibria from [1943Tro], [1967Hil], [1972Pre], and [1982Sri]. The equilibria between fcc-A12, bcc-A1 and cub-A13 phases were adopted from [1956Hel, 1990Mas]. Martensitic (fcc-A1/cph-A3) transformation temperatures (A_s and M_s) were taken from [1943Tro], [1966Ume], and [1995Cot, 1998Cot].

The calorimetric data of the enthalpy of formation of liquid and solid Fe-Mn alloys from [1974Bat, 1987Kub, 2003Wit] and the activity data of manganese in the liquid and solid alloys [1955San, 1961Bun, 1966Sch, 1967Sch, 1973Ste, 1974Ben, 1979Sud, 1984Jac, 1987Hay] were used. Heat capacity data and enthalpy of transformation data of both α-Fe-Mn and γ-Fe-Mn alloys were adopted from the most recent investigations of [2002Li] and [2003Wit]. The composition variations of the Curie and Néel temperatures of the phases were described by polynomials using the appropriate experimental data of [1966Ume, 1967Ish, 1967Has, 1971End, 2002Li, 2003Wit].

3. Thermodynamic Modeling

The Fe-Mn system contains the following solution phases [1956Hel, 1998COS]: liquid, bcc-A2, bcc-A12, cub-A13 and fcc-A1; a metastable cph-A3 phase has been also identified. All these phases can be described as substitutional solutions using the Redlich-Kister polynomial description for the corresponding Gibbs energies, as in previous assessments [1987Hua, 1989Hua, 1989Lee]. The molar Gibbs free energy of each phase (ϕ) listed can be expressed as:

$$G^{\phi} = x_{\mathrm{Fe}}\,{}^{0}G^{\phi}_{\mathrm{Fe}} + x_{\mathrm{Mn}}\,{}^{0}G^{\phi}_{\mathrm{Mn}} + G^{\phi}_{\mathrm{m}} + G^{\phi}_{\mathrm{mag}} \qquad \text{(Eq 1)}$$

Here ${}^{0}G^{\phi}_{i}$ is the Gibbs energy of a phase, ϕ, of a pure element i (i = Fe, Mn) relative to the Gibbs energy for its stable phase in the paramagnetic state at 298.15 K; x_i is the mole fraction of pure element i; G^{ϕ}_{m} is the molar Gibbs energy of mixing for phase ϕ; and G^{ϕ}_{mag} is the magnetic ordering energy (paramagnetic→(anti)ferromagnetic transition) of the phase ϕ. For the substitutional solution phase ϕ of the binary Fe-Mn system, the molar Gibbs energy of mixing is expressed as

$$G^{\phi}_{\mathrm{m}} = RT[x_{\mathrm{Fe}} \ln x_{\mathrm{Fe}} + x_{\mathrm{Mn}} \ln x_{\mathrm{Mn}}] + G^{\phi,\mathrm{s}} \qquad \text{(Eq 2)}$$

where R is the gas constant, T is the absolute temperature, and $G^{\phi,\mathrm{s}}$ is the molar excess Gibbs energy, which in terms of the empirical Redlich-Kister power series expansion is given by

---

V.T. Witusiewicz, ACCESS e.V., Intzestrasse 5, D-52072 Aachen, Germany; **F. Sommer** and **E.J. Mittemeijer,** Max Planck Institute for Metals Research, Heisenbergstrasse 3, D-70569 Stuttgart, Germany. Contact e-mail: f.sommer@mf.mpg.de.

$$G^{\phi,s} = x_{\mathrm{Fe}}\, x_{\mathrm{Mn}} \sum_{v=0}^{n} {}^{v}L^{\phi}_{\mathrm{Fe,Mn}}(x_{\mathrm{Fe}} - x_{\mathrm{Mn}})^{v} \qquad \text{(Eq 3)}$$

The temperature dependence of the model (fit) parameters ${}^{v}L^{\phi}_{\mathrm{Fe,Mn}}$ is described according to the CALPHAD convention as

$$\begin{aligned} {}^{v}L^{\phi}_{\mathrm{Fe,Mn}} &= a^{\phi}_{v} + b^{\phi}_{v}T + c^{\phi}_{v}T\ln T + d^{\phi}_{v}T^{2} + e^{\phi}_{v}T^{3} + f^{\phi}_{v}T^{-1} \\ &\quad + g^{\phi}_{v}T^{7} + h^{\phi}_{v}T^{-9} \qquad \text{(Eq 4)} \end{aligned}$$

with a to h as empirical parameters.

The magnetic contribution has been considered for bcc-A2 (ferromagnetic phase), fcc-A1, bcc-A12, and cph-A3 (antiferromagnetic phase). For these phases the magnetic ordering energy was modeled according to the CALPHAD approach [1991Din] in terms proposed by Hillert and Jarl [1978Hil]:

$$G^{\phi}_{\mathrm{mag}} = RT\ln(\beta^{\phi} + 1)g(\tau) \qquad \text{(Eq 5)}$$

with

$$g(\tau) = 1 - \left(\frac{79\tau^{-1}}{140p} + \frac{474}{497}\left(\frac{1}{p} - 1\right)\left(\frac{\tau^{3}}{6} + \frac{\tau^{9}}{135} + \frac{\tau^{15}}{600}\right)\right)/D \quad \text{if } \tau < 1$$

$$g(\tau) = -\left(\frac{\tau^{-5}}{10} + \frac{\tau^{-15}}{315} + \frac{\tau^{-25}}{1500}\right)/D \qquad \text{if } \tau > 1$$

$D = 0.46044 + 0.73189(1/(p - 1))$ and $\tau = T/T^{\phi}_{\mathrm{C,N}}$, where T^{ϕ}_{C} denotes the Curie temperature of the phase ϕ (ferromagnetic to paramagnetic transformation), T^{ϕ}_{N} denotes the Néel temperature of the phase ϕ (antiferromagnetic to paramagnetic transformation), and β^{ϕ} is the average magnetic moment per atom of phase ϕ. The value of p depends on the crystal structure. For the bcc-A2 phase $p = 0.40$, while for the fcc-A1, bcc-A12 and cph-A3 phases $p = 0.28$ [1991Din]. The magnetic contribution to the heat capacity from Eq 5 results in

$$C^{\phi}_{p_{\mathrm{mag}}} = R\ln(\beta^{\phi} + 1)\, c(\tau) \qquad \text{(Eq 6)}$$

with

$$c(\tau) = \left(\frac{474}{497}\left(\frac{1}{p} - 1\right)\left(2\tau^{3} + \frac{2\tau^{9}}{3} + \frac{2\tau^{15}}{5}\right)\right)/D \qquad \text{if } \tau < 1$$

and

$$c(\tau) = \left(2\tau^{-5} + \frac{2\tau^{-15}}{3} + \frac{2\tau^{-25}}{5}\right)/D \qquad \text{if } \tau > 1$$

The composition dependences of T^{ϕ}_{C} or T^{ϕ}_{N} and β^{ϕ} have been modeled as follows [1998COS]:

$$T^{\phi}_{\mathrm{C,N}}(x) = (x_{\mathrm{Fe}}T^{\phi}_{\mathrm{C,N,Fe}} + x_{\mathrm{Mn}}T^{\phi}_{\mathrm{N,Mn}}) + T^{\phi,s}_{\mathrm{C,N}} \qquad \text{(Eq 7)}$$

$$\beta^{\phi}(x) = (x_{\mathrm{Fe}}\beta^{\phi}_{\mathrm{Fe}} + x_{\mathrm{Mn}}\beta^{\phi}_{\mathrm{Mn}}) + \beta^{\phi,s} \qquad \text{(Eq 8)}$$

where deviations from the additive behavior of the component properties $T^{\phi,s}_{\mathrm{C,N}}$ and $\beta^{\phi,s}$ are both represented by also Redlich-Kister power series expansions, analogous to Eq 3. If Eq 7 and 8 result in negative values of $T^{\phi}_{\mathrm{C,N}}(x)$ and $\beta^{\phi}(x)$, it indicates that the phase ϕ is antiferromagnetic. The real values of $T^{\phi}_{\mathrm{C,N}}$ and β^{ϕ} are obtained by dividing $T^{\phi}_{\mathrm{C,N}}$ and β^{ϕ} calculated from Eq 7 and 8 by −1 for the bcc-A2 phase and −3 for the fcc_A1, bcc-A12, and cph-A3 phase [1989Hua].

The coefficients of the polynomials (Eq 3, 4, 7, 8) have been determined by fitting corresponding experimental information, referred to above, using the module Parrot in Thermo-Calc [1985Sun], which provides simultaneous fits to different types of thermodynamic data. The parameters thus derived in the present work have been gathered in Table 1. Obviously, for the cub-A13 and bcc-A12 phases the regular solution model provides agreeable fits ($\nu = 0$) (Eq 3), whereas the liquid, fcc-A1, bcc-A2, and cph-A3 phases had to be described by the subregular model ($\nu = 0{,}1$). To obtain a satisfactory representation of the experimental molar heat capacity data of the fcc-A1 phase of the Fe-Mn system [2003Wit] (Fig. 8) the coefficients a-e of Eq 4 had to be used. The thermodynamic data for the Gibbs energy of phases (${}^{0}G^{\phi}_{\mathrm{i}}$) and the magnetic parameters T^{ϕ}_{C}, T^{ϕ}_{N}, and β^{ϕ} of iron and manganese in the stable and metastable state were taken from the SGTE data base for pure elements [1991Din].

4. Results and Discussion

A comparison of the experimental and calculated data characterizing the invariant equilibria occurring in the Fe-

Table 1 Optimized Thermodynamic Model Parameters for the Phases of the Fe-Mn System (Eq 3,4,7 and 8); L in J mol^{-1} and T in K

Phase	Parameter	Value
Liquid	${}^{0}L^{\mathrm{liquid}}_{\mathrm{Fe,Mn}}$	$-2928.5 + 0.8779\,T$
	${}^{1}L^{\mathrm{liquid}}_{\mathrm{Fe,Mn}}$	$849.0 + 0.3832\,T$
bcc-A2	${}^{0}L^{\mathrm{bcc\text{-}A2}}_{\mathrm{Fe,Mn}}$	$-3940.1 + 3.1300\,T$
	${}^{1}L^{\mathrm{bcc\text{-}A2}}_{\mathrm{Fe,Mn}}$	$6405.3 - 3.8396\,T$
	${}^{0}T^{\mathrm{bcc\text{-}A2}}_{\mathrm{C(Fe,Mn)}}$	370
fcc-A1	${}^{0}L^{\mathrm{fcc\text{-}A1}}_{\mathrm{Fe,Mn}}$	$-13\,107.0 + 13.8608\,T + 0.9523\,T\ln T - 13.2532 \times 10^{-3}\,T^{2} + 3.2854 \cdot 10^{-6}\,T^{3}$
	${}^{0}T^{\mathrm{fcc\text{-}A1}}_{\mathrm{N(Fe,Mn)}}$	−2358
	${}^{1}T^{\mathrm{fcc\text{-}A1}}_{\mathrm{N(Fe,Mn)}}$	−1602
	${}^{0}\beta^{\mathrm{fcc\text{-}A1}}_{\mathrm{Fe,Mn}}$	2.872
	${}^{1}\beta^{\mathrm{fcc\text{-}A1}}_{\mathrm{Fe,Mn}}$	3.666
cub-A13	${}^{0}L^{\mathrm{cub\text{-}A13}}_{\mathrm{Fe,Mn}}$	$-10\,860.8 + 3.1408\,T$
bcc-A12	${}^{0}L^{\mathrm{bcc\text{-}A12}}_{\mathrm{Fe,Mn}}$	$-11\,848.9 + 2.6800\,T$
cph-A3	${}^{0}L^{\mathrm{cph\text{-}A3}}_{\mathrm{Fe,Mn}}$	$-10\,269.9 + 19.1867\,T$
	${}^{1}L^{\mathrm{cph\text{-}A3}}_{\mathrm{Fe,Mn}}$	−4117.7

Table 2 Calculated and Experimental Data for Characteristics of Invariant Equilibria in the Fe-Mn System

Type of Equilibrium and Reaction Between Phases ϕ_1, ϕ_2, and ϕ_3	Mole Fraction x_{Mn} ϕ_1	ϕ_2	ϕ_3	T/K	Reference	Remark
Eutectoid: cub-A13 ↔ fcc-A1 + bcc-A12	0.66 ± 0.03	0.62 ± 0.03	0.68 ± 0.03	973 ± 10	[1956Hel]	exp.
	0.701	0.590	0.703	973	[1987Hua]	calc.
	0.681	0.606	0.690	973	[1989Hua,1998COS]	calc.
	0.670	0.592	0.679	973.5	This work	calc.
Eutectoid: fcc-A1 ↔ bcc-A2 + bcc-A12 (a)	0.436	0.033	0.659	521	[1989Hua,1998COS]	calc.
	0.431	0.022	0.647	528	This work	calc.
Peritectic: liquid + bcc-A2 ↔ fcc-A1	0.130 ± 0.005	0.096 ± 0.005	0.102 ± 0.005	1747 ± 5	[1956Hel]	exp.
	0.130	0.101	0.102	1746	[1987Hua]	calc.
	0.129	0.100	0.101	1747	[1989Hua,1998COS]	calc.
	0.139	0.100	0.102	1748.5	This work	calc.
Peritectic: liquid + bcc-A2 ↔ fcc-A1	0.867 ± 0.017	0.870 ± 0.017	0.864 ± 0.017	1507 ± 5	[1956Hel]	exp.
	0.909	0.912	0.903	1508	[1987Hua]	calc.
	0.867	0.877	0.875	1507	[1989Hua,1998COS]	calc.
	0.877	0.878	0.868	1509.6	This work	calc.
Congruent point: fcc-A1 ↔ cub-A13	0.87 ± 0.03	0.87 ± 0.03	…	1429 ± 5	[1956Hel]	exp.
	0.863	0.863	…	1429	[1987Hua]	calc.
	0.864	0.864	…	1429	[1989Hua,1998COS]	calc.
	0.854	0.854	…	1433.2	This work	calc.

(a) No experimental data available

Mn system is provided in Table 2; results of the previous work [1987Hua, 1989Hua, 1998COS] have also been given in Table 2. The values given for temperatures and the compositions characterizing all invariant equilibria are reproduced within experimental error [1956Hel].

The stable and metastable phase diagrams as calculated according to the present reevaluation (solid lines) and according to the previous optimization (dotted lines) and the available experimental data (points) are shown in Fig. 1 and 2, respectively. The present optimization yields in a range from 5-10 K smaller deviations of temperatures of the liquid/fcc-A1 and the fcc-A1/cub-A13 equilibria from the experimental data than the assessment of [1989Hua] (see enlarged high temperature Fe-rich and Mn-rich parts in Fig. 1b and c, respectively). The limiting solubility of Mn in the low temperature bcc-A2 phase (Fig. 1a) is reproduced better as well. However, the most pronounced difference between the present and previous descriptions emerges at the Mn-rich part of the stable phase diagram (Fig. 1) and both sides of the equiatomic composition in the metastable phase diagram (Fig. 2). These distinctions are caused by the use of the recent experimental data for the enthalpy of formation and heat capacity of γ-Fe-Mn alloys [2003Wit] and for the martensitic/austenitic transformation temperatures [1995Cot, 1998Cot]. The solubility of Mn in the Fe-rich cph-A3 phase and of Fe in the Mn-rich cph-A3 phase decreases according to the present reevaluation with decreasing temperature (Fig. 2, solid lines). An abrupt change of the slope of these solubility lines in Fig. 2 occurs at composition at which the Néel temperature of the cph-A3 phase is equal to the temperature of the martensitic transformation ($T_N^{\text{cph-A3}} = M_s$).

The activity of manganese (Mn) in liquid alloys (standard states are liquid Fe and liquid Mn) and solid alloys (standard states are bcc-A1 Fe and cub-A13 Mn) is shown as a function of composition in Fig. 3. Horizontal parts of the activity function for the iron-rich alloys and for the manganese-rich alloys correspond to the bcc-A2/fcc-A1 phase transformation and the fcc-A1/cub-A13 phase transformation, respectively. In view of the experimental errors, both the present modeling and the previous modeling [1989Hua] reproduce the activity of Mn in the liquid and solid alloys. The calculated values of the activity match especially well the experimental data of Schultz et al. [1966Sch] (Fig. 3a) and Kubitz et al. [1987Hay] (Fig. 3b).

The enthalpy of mixing of liquid Fe-Mn alloys is shown as a function of composition in Fig. 4. The present description represents the most recent experimental results [2003Wit] and the data of [1974Bat] for dilute solutions. The values for H_m^l from [1974Bat] near the equiatomic composition are about 200 J mol^{-1} more negative than the calculated values. This discrepancy, in particular in the middle composition range, can be due to (a) the determination of the calibration factor of the calorimeter used in [1974Bat] only for (the initial amounts of) pure liquid Fe and pure liquid Mn; and (b) the additional supposition in [1974Bat] that this calibration factor be composition independent. This is not true, because upon reaching the equiatomic composition by successive addition of samples of alloying element to the (initially pure) melt, the volume of the liquid Fe-Mn alloy increases by a factor of two and the calibration factor varies proportionally.

The enthalpy of formation of solid γ-Fe-Mn alloys (with pure metastable fcc-A1 Fe and fcc-A1 Mn as reference states) is shown as a function of composition in Fig. 5. The calculated function agrees well with the most recent experimental values [2003Wit]. At the equiatomic composition the calculated value is about 1000 J mol^{-1} less negative than data provided by [1987Kub]. It should be mentioned that the

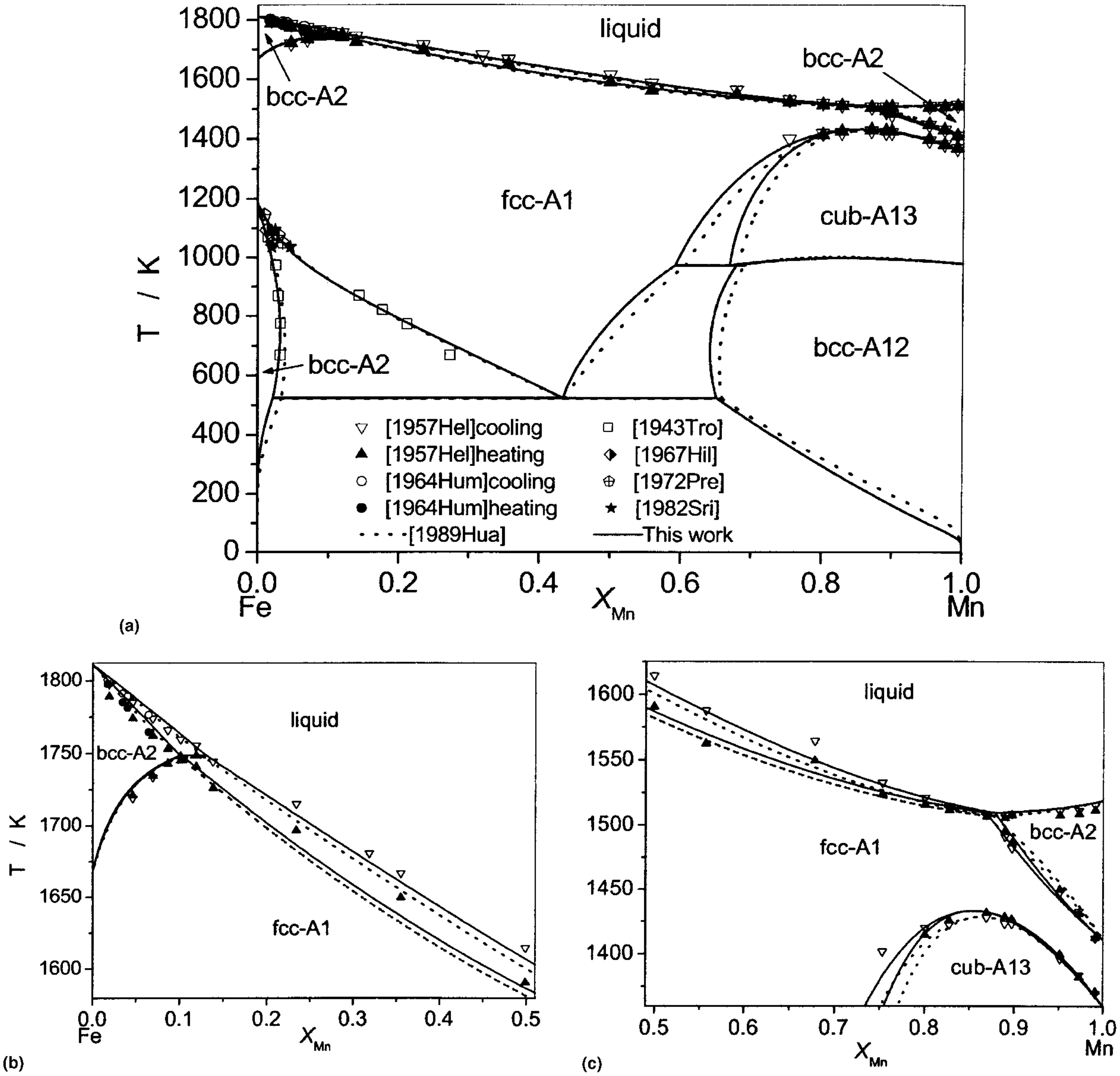

Fig. 1 Phase diagram of the Fe-Mn system: solid lines result from the evaluated parameters of present work; dotted lines result from the evaluation of [1989Hua]. Experimental data have been indicated (points).

enthalpy of formation of [1987Kub] were corrected for the heat content of pure iron according to the most recent heat capacity data of pure iron provided by [2003Wit].

The enthalpy content of the γ-Fe-Mn alloys at 1409 K versus mole fraction of Mn is shown in Fig. 6. The present description matches the experimental points well, whereas the preceding optimization [1989Hua] results in an unsatisfactory match.

The experimental and calculated temperature and composition variations of the heat capacity of solid α-Fe-Mn and solid γ-Fe-Mn are shown in Fig. 7 and 8, respectively. Though the outcome is not fully satisfactory, the current evaluation provides a better fit to the experimental data (solid lines) than the previous assessment [1989Hua] (dotted lines) particularly for γ-Fe-Mn alloys (Fig. 8) due to the use of the five first terms of Eq 4. The discrepancies observed between our calculated value and experimental values are caused mainly by inadequate description of the magnetic contribution according to Eq 5-8, and as implemented in the CALPHAD software [1985Sun].

Therefore a new representation of the magnetic ordering energy is presented. The magnetic contribution C^{ϕ}_{pmag} for both the bcc-A2 phase and the fcc-A1 phase for the Fe-Mn system can be well described, i.e., within experimental error, by the following equation

$$C^{\phi}_{\mathrm{pmag}} = aR \ln(\beta^{\phi} + 1) \exp(-5\tau)\tau^{-(1/5a)} \qquad \text{(Eq 9)}$$

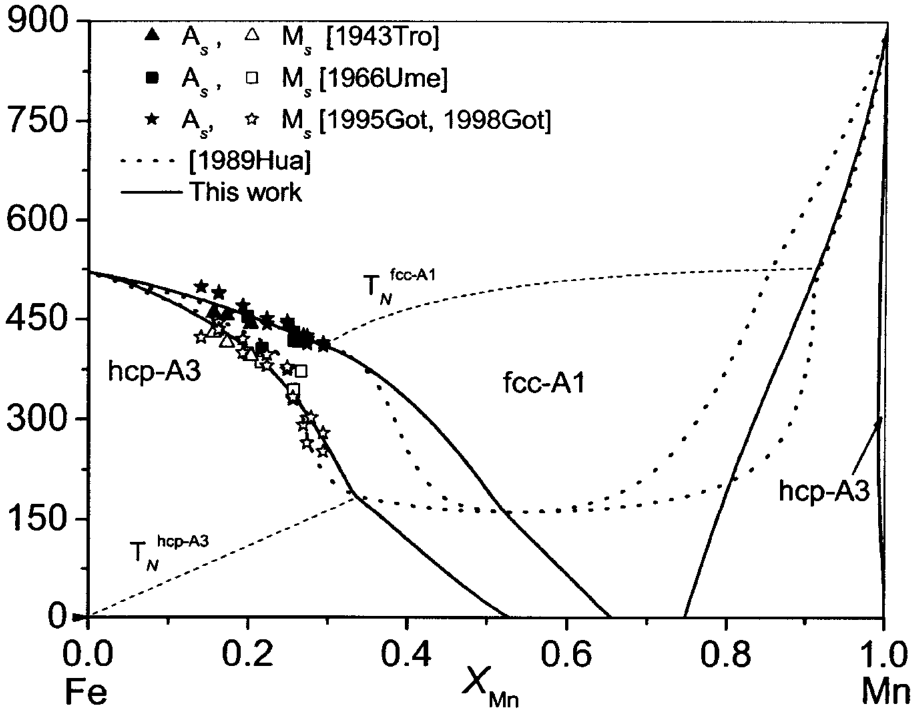

Fig. 2 Metastable phase diagram of the Fe-Mn system: solid lines for temperatures of the austenitic (A_s) and the martensitic (M_s) transformations result from present assessment, dotted lines result from [1989Hua], points are experimental data and dashed lines indicate Néel temperatures of the phases.

with $a = 2$ if $T < T_{C,N}$ and $a = 1$ if $T > T_{C,N}$, where $\tau = |T/T_{C,N} - 1|$.

This representation is equivalent to the relation recently proposed by [2002Kem] $C_p = h \exp(-k\tau)\tau^{-m}$ with $h = aR \ln(\beta^\phi + 1)$, $k = 5$ and $m = 1/5a$.

Using Eq 9 and expanding the heat capacity of the Fe-Mn alloys by

$$C_p^\phi = x_{Fe}\, C_{pFe}^{\phi,paramag} + x_{Mn}\, C_{pMn}^{\phi,paramag} + C_p^{\phi,paramag,ex} + C_{pmag}^\phi \qquad \text{(Eq 10)}$$

the following parameters were obtained for the heat capacity of the α-Fe-Mn alloys (bcc-A2 phase) on the basis of data presented in [2002Li]:

$$C_p^{bcc-A2,paramag,ex} = 68.7\, x_{Fe}x_{Mn} \quad (\text{J mol}^{-1}\ \text{K}^{-1}) \qquad \text{(Eq 11)}$$

$$\beta^{bcc-A2} = 2.22x_{Fe} + 0.27x_{Mn} - 14.8x_{Fe}x_{Mn} \qquad \text{(Eq 12)}$$

$$T_{C,N}^{bcc-A2} = 1043x_{Fe} + 580x_{Mn} - 832x_{Fe}x_{Mn} \quad (\text{K}) \qquad \text{(Eq 13)}$$

and for the heat capacity of the γ-Fe-Mn alloys (fcc-A1 phase) on the basis of data presented in [2003Wit]:

$$C_p^{fcc-A1,paramag,ex} = x_{Fe}x_{Mn}[9.5 - 28.4(x_{Fe} - x_{Mn})^2 + 1.38 \times 10^{-2}T - 1.60 \times 10^{-5}T^2] \quad (\text{J mol}^{-1}\ \text{K}^{-1}) \qquad \text{(Eq 14)}$$

$$\beta^{fcc-A1} = 0.70x_{Fe} + 0.62x_{Mn} + x_{Fe}x_{Mn}[-1.15 - 0.90(x_{Fe} - x_{Mn})] \qquad \text{(Eq 15)}$$

$$T_N^{fcc-A1} = 67x_{Fe} + 540x_{Mn} + x_{Fe}x_{Mn}[786 + 534(x_{Fe} - x_{Mn})] \quad (\text{K}) \qquad \text{(Eq 16)}$$

The appropriate values on heat capacity of pure elements in the paramagnetic state ($C_{pFe}^{bcc-A2,paramag}$, $C_{pMn}^{bcc-A2,paramag}$, $C_{pFe}^{fcc-A1,paramag}$, and $C_{pMn}^{fcc-A1,paramag}$) were adopted from the SGTE database [1991Din]. The descriptions thus attained for the heat capacity of the α- and γ-Fe-Mn alloys are also shown in Fig. 7 and 8. Indeed, Eq 9-16 provide much better fits to the experimental data than Eq 5-8. Unfortunately, a direct implementation of Eq 9-16 in the Poly-3 and Parrot modules of the commercial Thermo-Calc program [1985Sun] cannot be realized by the Thermo-Calc user.

5. Conclusions

The CALPHAD description of Fe-Mn alloy system was updated in the following ways.

- New experimental results for the enthalpy of mixing of liquid Fe-Mn alloys, the enthalpy of formation of γ-Fe-Mn solid solutions, the heat capacity of solid α-Fe-Mn

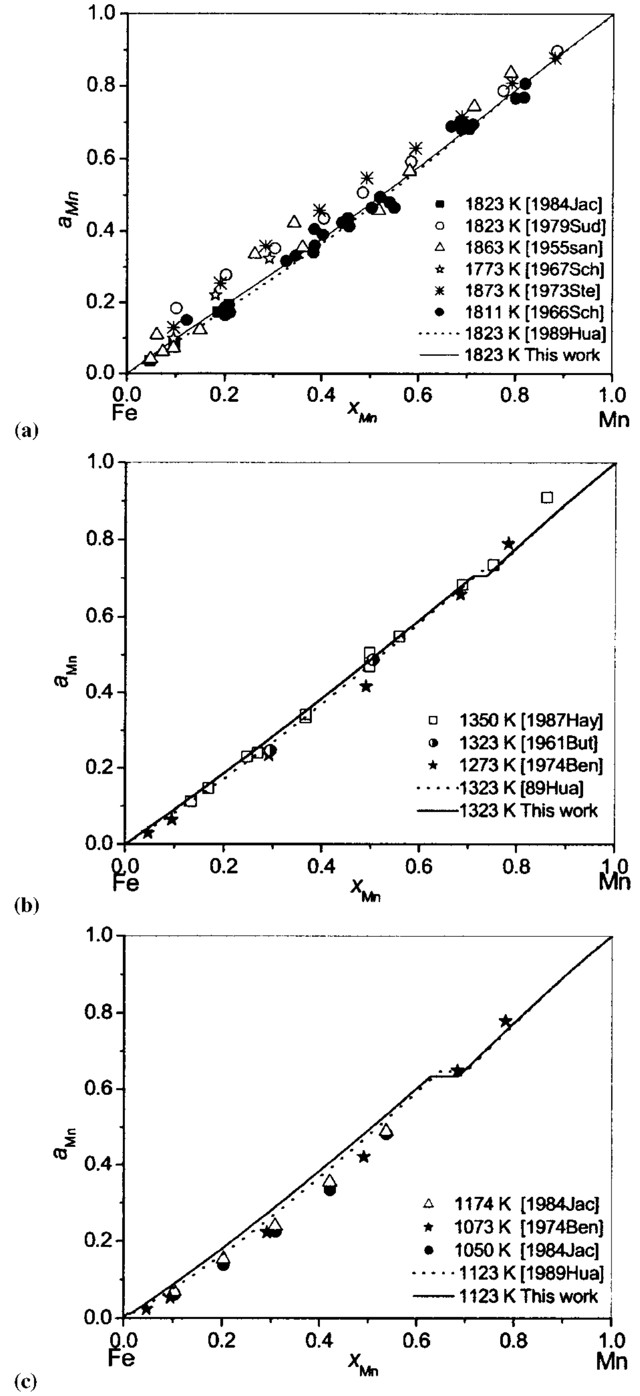

Fig. 3 Activity of Mn in the Fe-Mn alloys at different temperatures: (**a**) for liquid alloys relative to liquid components, (**b**) and (**c**) for solid alloys relative to bcc-A2 Fe and cub-A13 Mn, points are experimental data, solid lines result from present evaluation and dotted lines result from evaluation of [1989Hua].

and γ-Fe-Mn alloys necessitate an update of the CALPHAD description of the Fe-Mn system (phase diagrams and thermodynamic properties).

- The reevaluation of the phase equilibria and thermodynamic functions leads to consistently better fits to the available experimental data.

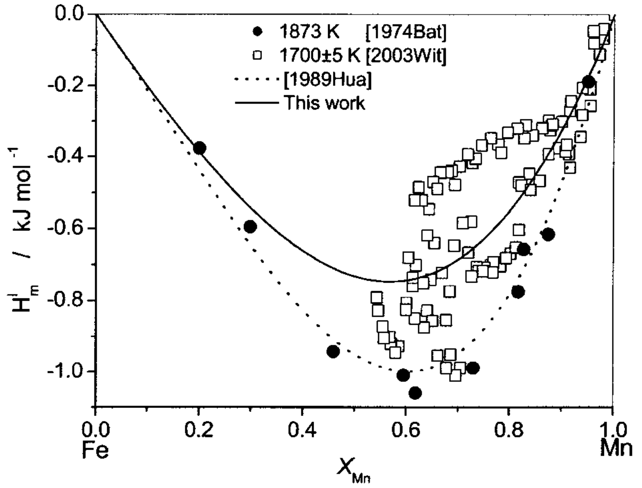

Fig. 4 Integral enthalpy of mixing of liquid Fe-Mn alloys [1974Bat, 2003Wit]: solid line results from present assessment, dotted line results from [1989Hua] and points are experimental data.

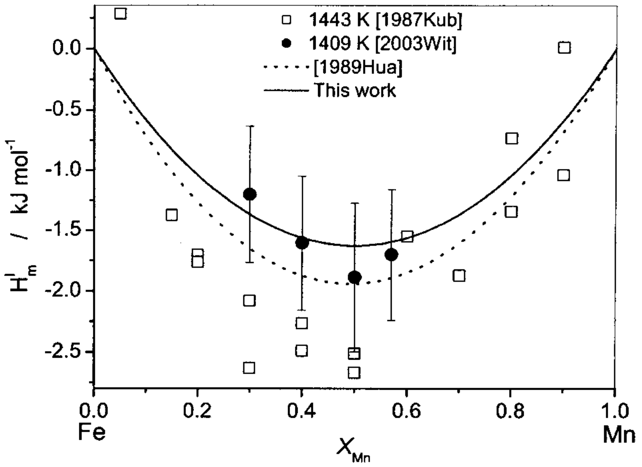

Fig. 5 The enthalpy of formation of solid γ-Fe-Mn alloys with reference to metastable fcc-A1 Fe and fcc-A1 Mn: solid line results from present assessment at temperature 1409 K, dotted line results from the assessment by [1989Hua] and points are experimental values.

- A new description for the magnetic contribution of the heat capacity of ferromagnetic and antiferromagnetic phases in the Fe-Mn system is proposed that leads to much better representation of the temperature dependence of C_p than the approach implemented in the CALPHAD software.

References

1943Tro: A.R. Troiano and F.T. McGuire: "A Study of the Iron-Rich Iron-Manganese Alloys," *Trans. ASM,* 1943, *31,* pp. 340-59.

1955San: K. Sanongi and M. Ohtani: "On the Activity of Coexisting Elements in Molten Iron. III. The Activity of Mn Molten

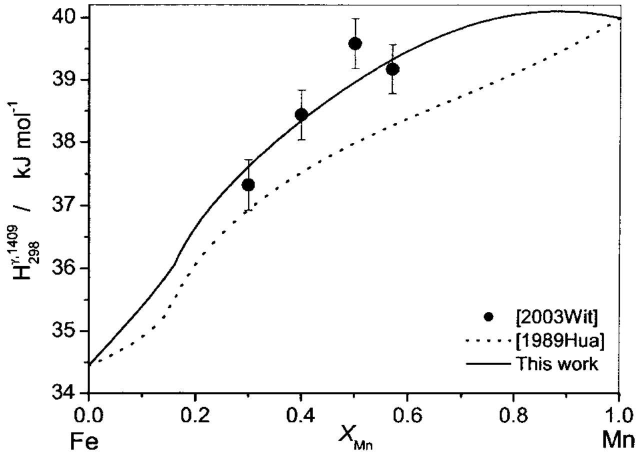

Fig. 6 The enthalpy content upon heating from 298-1409 K of the stable and metastable γ-Fe-Mn alloys versus mole fraction of manganese: the solid line results from the present assessment, the dotted line results from [1989Hua] and points are experimental values [2003Wit].

Fe-Mn Alloys," *Sci. Rep. Res. Inst. Tohoku Uni. A,* 1955, *7,* pp. 201-09.

1956Hel: A. Hellawell: "The Equilibrium Diagram of the System Iron-Manganese," Annotated Equilibrium Diagrams, No. 26, The Inst. Met., London, UK, 1956.

1957Hel: A. Hellawell and W. Hume-Rothery: "The Constitution of Alloys of Iron and Manganese with Transition Elements of the First Long Period," *Philos. Trans., Royal Soc. London,* 1957, *249,* pp. 417-59.

1961But: J.F. Butler, C.L. McCabe, and H.W. Paxton: "Thermodynamic Activities in the Fe-Mn-C System," *Trans. Met. Soc. AIME,* 1961, *221,* pp. 479-84.

1966Ume: H. Umebayashi and Y. Ishikawa: "Antiferromagnetism of γ-Fe-Mn Alloys," *J. Phys. Soc. Jpn.,* 1966, *21,* pp. 1281-94.

1966Sch: C.W. Schultz, W. Riazance, and S.L. Payne: "Activity of Manganese in Liquid Iron-Manganese Alloys," *US Bureau of Mines, Rep. Investigation,* 1966, R.I. 6807.

1967Has: T. Hashimoto and Y. Ishikawa: "Antiferromagnetism of γ-Fe-Mn Alloys. III. Specific Heat and Thermoelectric Power Studies," *J. Phys. Soc. Jpn.,* 1967, *23,* pp. 213-23.

1967Hil: M. Hillert, T. Wada, and H. Wada: "The α→γ Equilibrium in Fe-Mn, Fe-Mo, Fe-Ni, Fe-Sb, Fe-Sn and Fe-W Systems," *J. Iron Steel Inst.,* 1967, *205,* pp. 539-46.

1967Ish: Y. Ishikawa and Y. Endoh: "Antiferromagnetism of

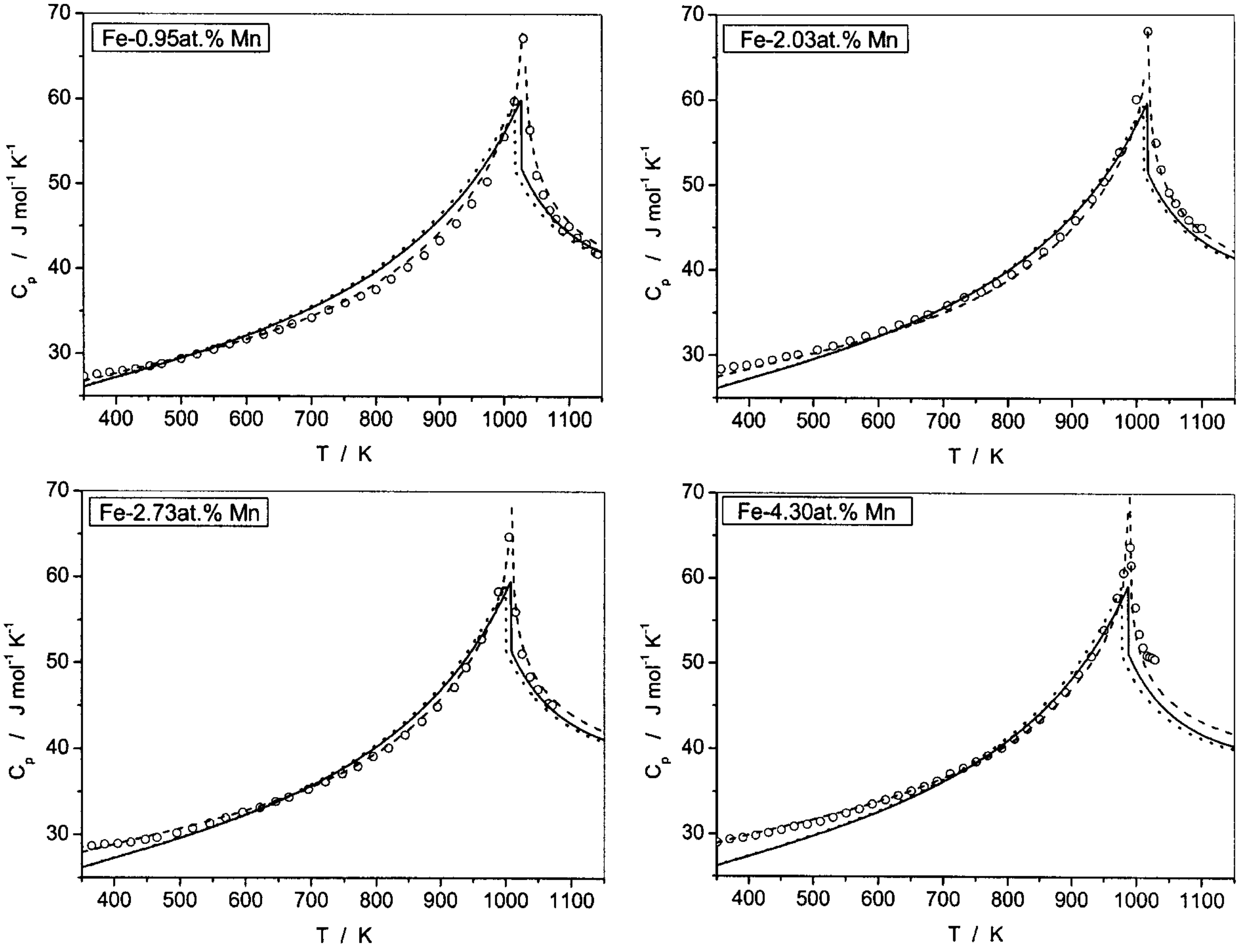

Fig. 7 Heat capacity of α-Fe-Mn alloys: solid lines result of calculation using the parameters given in Table 1, dotted lines result from description of [1989Hua], dashed lines result from Eq (9-13), and points are experimental data [2002Li, 2003Wit].

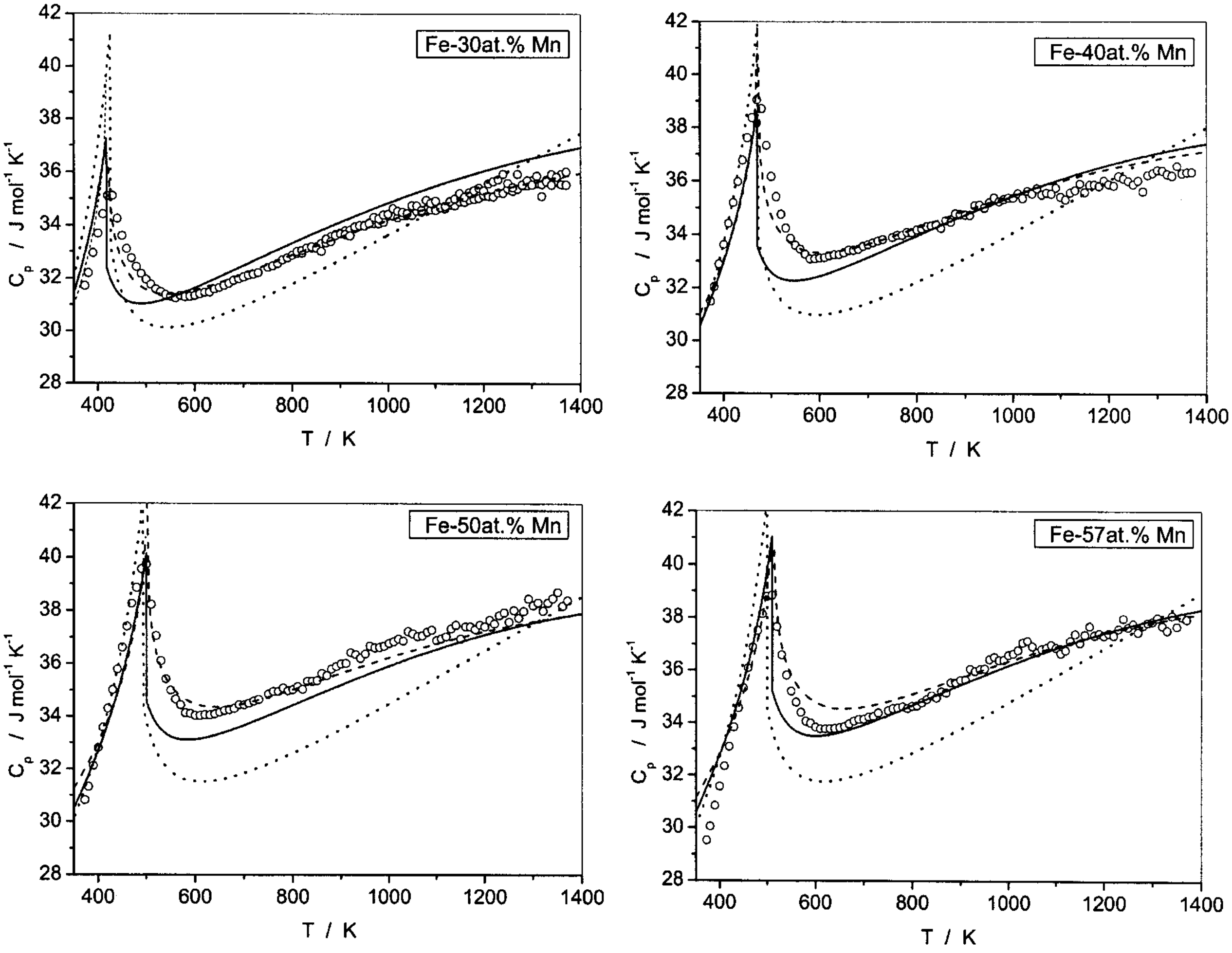

Fig. 8 Heat capacity of γ-Fe-Mn alloys: solid lines result of calculation using the parameters given in Table 1, dotted lines result from description of [1989Hua], dashed lines result from Eq 9, 10, 14-16, and points are experimental data [2003Wit].

γ-Fe-Mn Alloys. II. Neutron Diffraction and Mössbauer Effect Studies," *J. Phys. Soc. Jpn.,* 1967, *23,* pp. 205-13.

1967Sch: K. Schwerdtfeger: "Measurements of Oxygen Activity in γ-Iron, Iron-Silicon, Manganese and Iron-Manganese Melts Using Solid Electrolyte Galvanic Cell," *Trans. Met. Soc. AIME,* 1967, *239,* pp. 1276-80.

1971End: Y. Endoh and Y. Ishikawa: "Antiferromagnetism of γ-Iron-Manganese Alloys," *J. Phys. Soc. Jpn.,* 1971, *30,* pp. 1614-27.

1972Pre: B. Predel and W. Gust: "Ausscheidungsreaktionen im System Eisen-Mangan," *Arch. Eisenhuettenw.,* 1972, *43,* p. 721 (in German).

1973Ste: J.-M. Steiler, P. Ribond, M. Onilon, and M. Olette: "Détermination de l'activite thermodynamique des constituants du systems Fe-Mn liquide par une metode d'entrainement," *C.R. Acad. Sc. Paris,* 1973, *277C,* pp. 1207-10.

1974Bat: G.I. Batalin, N.N. Minenko, and V.S. Sudavtsova: "Enthalpy of Mixing and Thermodynamic Properties of Liquid Alloys of Iron with Manganese, Cobalt, and Nickel," *Russ. Metall.,* 1974, *5,* pp. 82-86.

1974Ben: R. Benz: "Thermodynamics of the Fe-Mn-C System from Solid State EMF Measurements," *Met. Trans.,* 1974, *5,* pp. 2217-19.

1978Hil: M. Hillert and M. Jarl: "A Model for Alloying Effects in Ferromagnetic Metals," *Calphad,* 1978, *2,* pp. 227-38.

1979Sud: V.S. Sudavtsova, G.I. Batalin, and V.A. Bandur: "Thermodynamic Properties of Liquid Alloys of the Fe-Mn System," *Ukr. Khim. Zhurn.,* 1979, *45,* pp. 718-21 (in Russian).

1982Sri: K.K. Srivastava and J.S. Kirkadly: "The Alpha-Gamma Phase Boundary and the T_0 Line for Fe-Mn Alloys," *Met. Trans.,* 1982, *13A,* pp. 2113-19.

1984Jac: K.T. Jacobs, P.J. Hajra, and M. Iwase: "Activities of Mn in Solid and Liquid Fe-Mn Alloys," *Arch. Eisenhüttenwes.,* 1984, *55,* pp. 421-26

1985Sun: B. Sundman, B. Jansson, and J.O. Andersson: "The Thermo-Calc Databank System," *Calphad,* 1985, *9,* pp. 153-90.

1987Hua: W. Huang: "An Assessment of the Fe-Mn System," *Calphad,* 1987, *11,* pp. 183-86.

1987Kub: R. Kubitz and F.H. Hayes: "Enthalpies of Mixing in the Iron-Manganese System by Direct Reaction Calorimetry," *Monatsh. Chem.,* 1987, *118,* pp. 31-41.

1987Hay: R. Kubitz, G. McHugh, and F.H. Hayes: "Calorimetric and Torsion Effusion Studies of Solid Fe-Mn Alloy," Dep. Metall. Mat. Sci., Univ. Manchester & U.M.I.S.T., Britain, 1987.

19879Hua: W. Huang: "An Assessment of the Fe-Mn System," *Calphad,* 1989, *13,* pp. 243-52.

1989Lee: B.-J. Lee and D.N. Lee: "A Thermodynamic Study on the Mn-C and Fe-Mn Systems," *Calphad,* 1989, *13,* pp. 345-54.

1990Mas: T.B. Massalski, H. Okamoto, P.R. Subramanin, and L. Kacprzak: *Binary Alloy Phase Diagrams,* 2nd ed., ASM International, Materials Park, OH, 1990.

1991Din: A.T. Dinsdale: "SGTE Data for Pure Elements," *Calphad,* 1991, *15,* pp. 317-425.

1995Cot: S. Cotes, M. Sade, and A. Fernández Guillermet: "Fcc/Hcp Martensitic Transformation in the Fe-Mn System: Experimental Study and Thermodynamic Analysis of Phase Stability," *Met. Trans.,* 1995, *26A,* pp. 1957-69.

1998COS: I. Ansara, A.T. Dinsdale, and M.H. Rand, ed.: COST 507. Definition of Thermophysical Properties to Provide a Database for the Development of New Light Alloys. Thermochemical Database for Light Metal Alloys. Vol. 2., Scientific Group Thermodata Europe Database, EUR 18499 en, 1998.

1998Cot: S. Cotes, A. Fernández Guillermet, and M. Sade: "Phase Stability and Fcc/Hcp Martensitic Transformation in Fe-Mn-Si Alloys: Part II. Thermodynamic Modeling of the Driving Forces and the M_s and A_s Temperatures," *J. Alloys Comp.,* 1998, *280,* pp. 168-77.

2002Li: C.-M. Li, F. Sommer, and E.J. Mittemeijer: "Characteristics of the $\alpha \rightarrow \gamma$ Transformation in Fe-Mn Alloys," *Mater. Sci. Eng.,* 2002, *325A,* pp. 307-19.

2002Kem: A.T.W. Kempen, F. Sommer, and E.J. Mittemeijer: "Calibration and Desmearing of a Differential Analysis Measurement Signal upon Heating and Cooling," *Thermochim. Acta,* 2002, *382,* pp. 21-30.

2003Wit: V.T. Witusiewicz, F. Sommer, and E.J. Mittemeijer: "Enthalpy of Formation and Heat Capacity of Fe-Mn Alloys," *Met. Trans.,* 2003, *34B,* pp. 209-23.